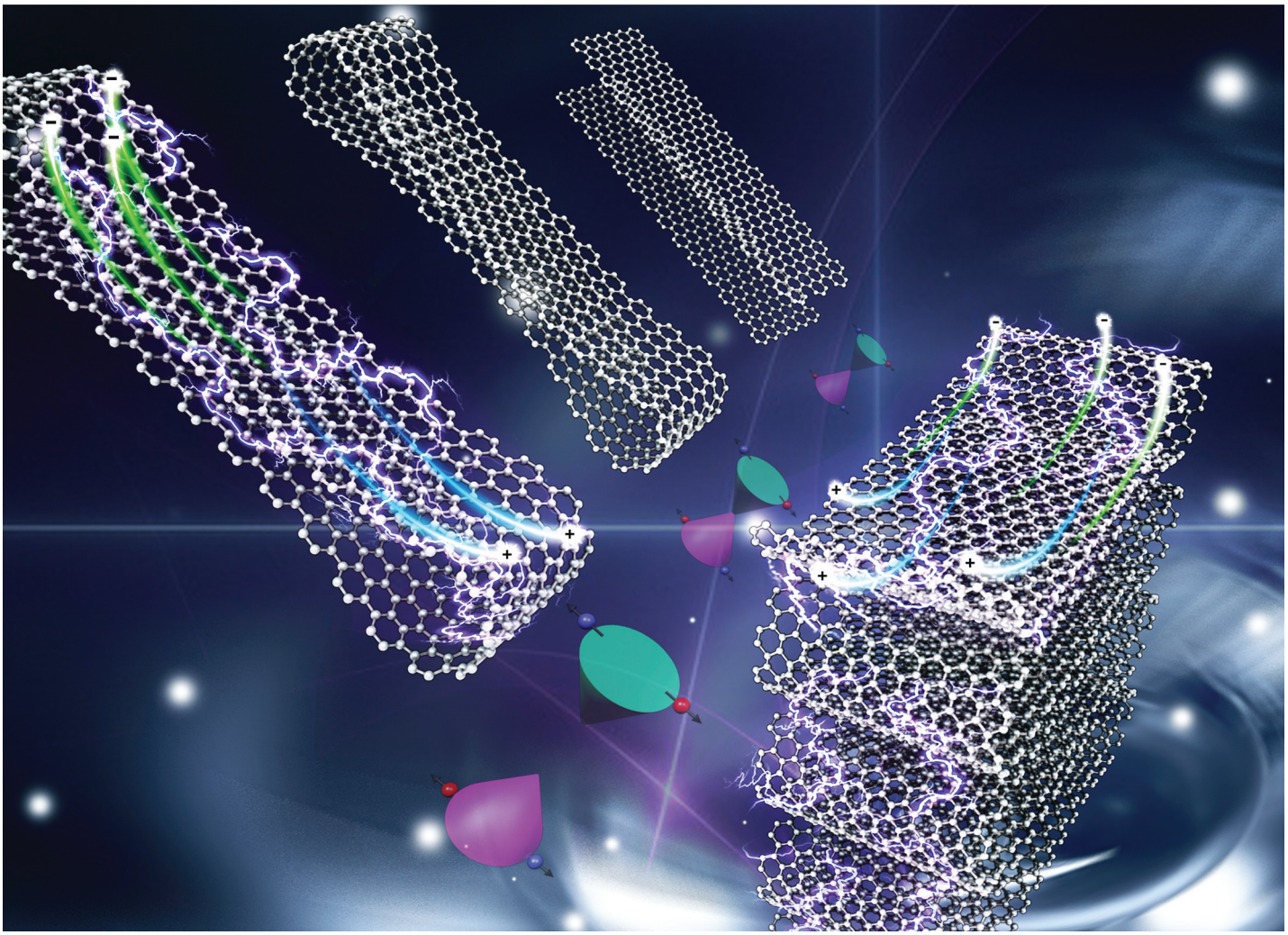

Showcasing research from the Division of Physics and Applied Physics, School of Physical and Mathematical Sciences, Nanyang Technological University, Singapore.

Title: Graphene homojunction: closed-edge bilayer graphene by pseudospin interaction

By properly closing graphene edges, two critical features of a junction, *i.e.* bandgap opening and spatial charge separation, can be realized in graphene. Such a graphene diode may play a role in future pseudospin electronics, such as for harvesting solar energy.

As featured in:

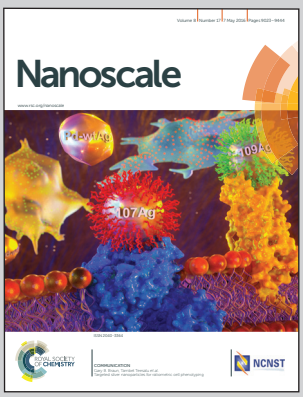

See Lei Liu, Zexiang Shen *et al.* *Nanoscale*, 2016, **8**, 9102.

ROYAL SOCIETY OF CHEMISTRY

www.rsc.org/nanoscale

Registered charity number: 207890

Nanoscale

COMMUNICATION

View Article Online
View Journal | View Issue

Cite this: *Nanoscale*, 2016, **8**, 9102

Received 16th November 2015,
Accepted 7th January 2016

DOI: 10.1039/c5nr08083e

www.rsc.org/nanoscale

Graphene homojunction: closed-edge bilayer graphene by pseudospin interaction

Jiaxu Yan,[a] Chao Li,[b] Da Zhan,[a] Lei Liu,*[c] Dezhen Shen,[c] Jer-Lai Kuo,[d] Shoushun Chen[e] and Zexiang Shen*[a]

Depending on the sublattices they are propagated in, low-energy electrons or holes are labeled with pseudospin. By engineering pseudospin interactions, we propose that two critical features of a junction, *i.e.*, band gap opening and spatial charge separation, can be realized in graphene layers with proper stacking. We also demonstrate theoretically that such a graphene diode may play a role in future pseudospin electronics such as for harvesting solar energy.

So far, many methods have been developed to open the band gap of graphene, including hydrogenation,[1] electrically gated bilayer graphene,[2–4] nanoribbons,[5,6] defects,[7] graphene-substrate interactions,[8] and absorption of molecules.[9] However, these methods also bring about unpleasant side effects in graphene after band gap opening, such as a dramatically increased effective mass, distorted lattice, and damaged layer integrity.[10] With such side effects, the resulting graphene will lose its superior transport performance. Another question when making electronic or optoelectronic devices from graphene is how to obtain p–n junctions. As graphene is normally p-doped by adsorbates, it is rather hard for it to be n-doped at the same time.[11] Although this problem seems to be solved by controlling the chemical bonding of the edges of graphene nanoribbons,[11] it would be much more desirable to separate electrons and holes in a more direct and efficient way for device applications. Recently, Liu *et al.* reported a novel graphene structure in which edge-opened AB-stacked bilayer graphene is transformed into an edge-closed AA-stacked structure after annealing at extremely high temperatures.[12] We also experimentally discovered that the zig-zag edges of AB-stacked bilayer graphene can easily form a closed structure even under low-temperature annealing conditions.[13] In this paper, we further demonstrate theoretically that both obstacles that hinder the electronics applications of graphene can be overcome by properly closing graphene edges.

The equivalence of atoms in the graphene unit cell leads its bonding (π) and anti-bonding (π^*) orbitals to touch each other at opposite corners of the Brillouin zone of K and K' and also gives an extra degree of freedom (*i.e.*, pseudospin) to its low-energy (LE) quasi-particles, as shown schematically in Fig. 1a. As they are an elementary property, real spins in graphene are invariant under overall morphological changes. However, as a direct result of the lattice symmetry of graphene, pseudospins have to comply with the chiral alignment of the graphene

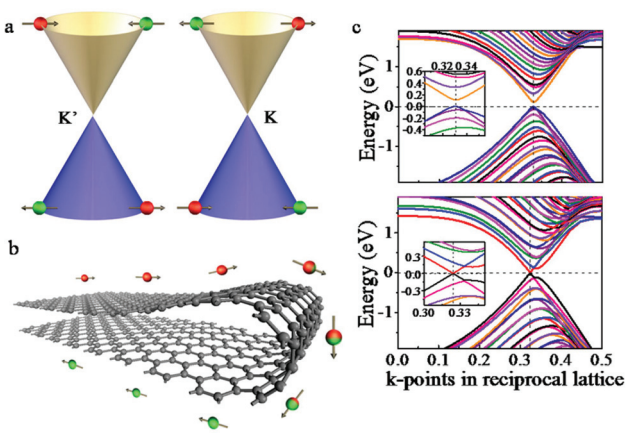

Fig. 1 (color online). (a) Schematic of LE electronic band structure of graphene. (b) Graphene layer with AB stacking folded along zig-zag edge. The red (green) balls with rightward (leftward) pointers represent pseudospin up (down). Only the right-hand part of the supercell is shown in each case. (c) Calculated band structures of AB-stacked (top) and AA-stacked CEBG (bottom). Insets: Magnification of the band gap regions. k is along the Γ–K direction in units of $2\pi/a$ (a is the lattice constant of graphene).

[a]*Division of Physics and Applied Physics, School of Physical and Mathematical Sciences, Nanyang Technological University, Singapore 637371, Singapore. E-mail: zexiang@ntu.edu.sg*
[b]*College of Physics, Jilin University, Changchun 130012, People's Republic of China*
[c]*Key Laboratory of Excited State Processes, Changchun Institute of Optics, Fine Mechanics and Physics, Chinese Academy of Sciences, Changchun 130033, People's Republic of China. E-mail: liulei@ciomp.ac.cn*
[d]*Institute of Atomic and Molecular Sciences, Academia Sinica, Taipei 10617, Taiwan*
[e]*School of Electrical and Electronic Engineering, Nanyang Technological University, Singapore 639798, Singapore*

sheet and therefore behave differently. For example, after closing its edges, its top and bottom layers may not have the same pseudospin chirality, such as the AB-stacked case shown in Fig. 1b. As the effect of pseudospin interactions has been extensively studied by now,[14–17] the study of the consequent electronic behaviors of graphene would be fundamentally meaningful for pseudospin physics.

In this work, a periodic AB-stacked closed-edge bilayer graphene (CEBG), as shown in Fig. 1a, was selected to investigate the interlayer pseudospin interactions. In this model, the interlayer distance for the three central carbon hexagons of CEBG was fixed at 3.4 Å, which is the typical layer distance of graphite. First-principles density functional theory calculations were carried out using the Vienna *ab initio* simulation package (VASP).[18–20] Electron-ion interactions were described using the projector augmented wave method and the exchange correlation potential using the generalized gradient approximation (GGA) in the Perdew–Burke–Ernzerhof form.[21] The cut-off energy for the basis set was 400 eV. Brillouin zone integration was performed within the Monkhorst–Pack scheme using a (24 × 1 × 1) mesh and Methfessel–Paxton smearing with a width of 0.2 eV. Model structures containing 120 carbon atoms were optimized with the vacuum separation set to be more than 10 Å, the interlayer distance for the three central carbon hexagons fixed at 3.4 Å, and the total energy converged to 1 meV. Fig. 1c plots the calculated band structure of CEBG, which presents the expected band gap of 0.113 eV at $k \approx 0.33$. The band gap of AB-stacked CEBG is crucial, as bilayer graphene is always metallic regardless of its stacking. As the finite curvature of graphene sheets may also induce energy gaps, such as in carbon nanotubes,[22] the role of curved edges in the band gap opening of AB-stacked CEBG was examined as well. For comparison, we evaluated edge effects by studying the band structure of the same CEBG model structure, but with AA stacking. As both top and bottom layers in AA-stacked CEBG display the same chirality, the interlayer pseudospin scattering in AA-stacked CEBG will vanish. As shown in Fig. 1a, the conduction band and valence band of AA-stacked CEBG intersect at the Dirac point without exhibiting band gap opening. Thus, the contribution of curved edges can be eliminated.

We then used the recently developed van der Waals density functional (vdW-DF),[23] which includes long-range dispersion interactions, to investigate the nature of the interlayer bonding in our CEBG models. The optimized geometries using vdW-DF are relatively similar to those from DFT calculations except for some increases in the interlayer distance in both cases (AA stacking: 3.759 Å; AB stacking: 3.632 Å). More importantly, as well as DFT calculations, vdW-DF calculations give a small gap (0.1 eV) for AB stacking and a gapless situation for AA stacking. We compared the difference in energy between AB- and AA-stacked models containing 32 carbon atoms. As expected, the total energy of AB stacking was 0.27 eV per cell lower than that of AA stacking. Next, we examined the robustness of our results with respect to a more rigorous approach such as the GW approximation.[24] G_0W_0 calculations were performed with the YAMBO code.[25] An affordable supercell containing 32 carbon atoms was adopted. Norm-conserving pseudopotentials were expanded on a plane-wave basis with an energy cut-off of 60 Ry. We chose a 64 × 1 × 1 *k*-point sample. The DFT and GW quasi-particle band structures of our CEBG models close to the Dirac point are shown in Fig. 2. As expected, for AA stacking there is still no gap, although GW self-energy corrections usually enlarge the gap. For AB stacking, the quasi-particle band structure has a significantly larger band gap (0.7 eV) instead of the DFT value of 0.3 eV, which is compared to that of bulk Ge (0.67 eV). Note that although the supercell studied here was quite small, the conclusion still holds for larger cases. When we considered the Coulomb truncation, for AA stacking there was still no gap, whereas for AB stacking the quasi-particle band gap (0.5 eV) with the Coulomb truncation is compared to that without the Coulomb truncation (0.7 eV). Therefore, our previous finding, independently of the level of sophistication, is arguably convincing and sheds new light on graphene research.

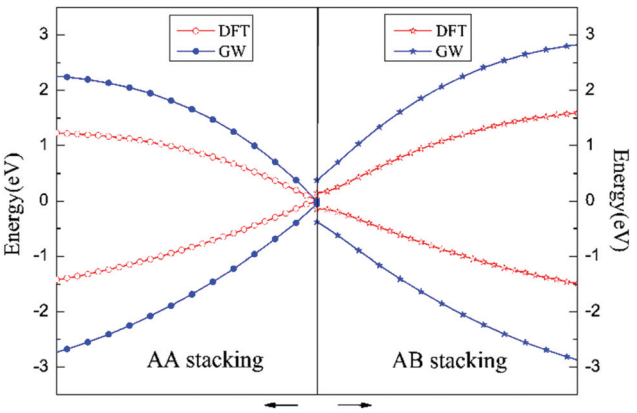

Fig. 2 (color online). DFT eigenvalues (hollow line) and GW quasi-particle energies (solid line) of AA-stacked and AB-stacked CEBG close to the Dirac point.

We constructed an effective tight-binding (TB) model to describe the low-energy physics based on the bases $\{p_z, s\}$, where we adopted one p_z projection on each carbon atom and one *s*-like projection in the middle of each bond.

$$H_{\mathrm{TB}} = \sum_{i,\alpha} \varepsilon_i^{\alpha} c_i^{\alpha+} c_i^{\alpha} + \sum_{\langle i,j\rangle,\alpha,\beta} t_{ij}^{\alpha\beta} (c_i^{\alpha+} c_j^{\beta} + \mathrm{h.c.})$$

Here, ε_i^{α} represents the on-site energy and $c_i^{\alpha+}$ (c_i^{α}) is the creation (annihilation) operator of electrons at site *i*. By fitting to the DFT data, we obtained a series of $t_{\mathrm{ij}}^{\alpha\beta}$ hopping parameters. As shown in Fig. 3, the TB model reproduces the low-energy bands well. Clearly, the energy spectrum is gapless in AA-stacked CEBG but has a finite gap in AB-stacked CEBG. Therefore, for band gap opening in AB-stacked CEBG, the band gap opening effect arises from pseudospin interactions only for closed edges. It is worth noting that band gap opening in AB-stacked CEBG originates from a new mechanism, which is not suitable for pristine open-edge bilayer graphene or graphite. For open-edge bilayer graphene or graphite, the

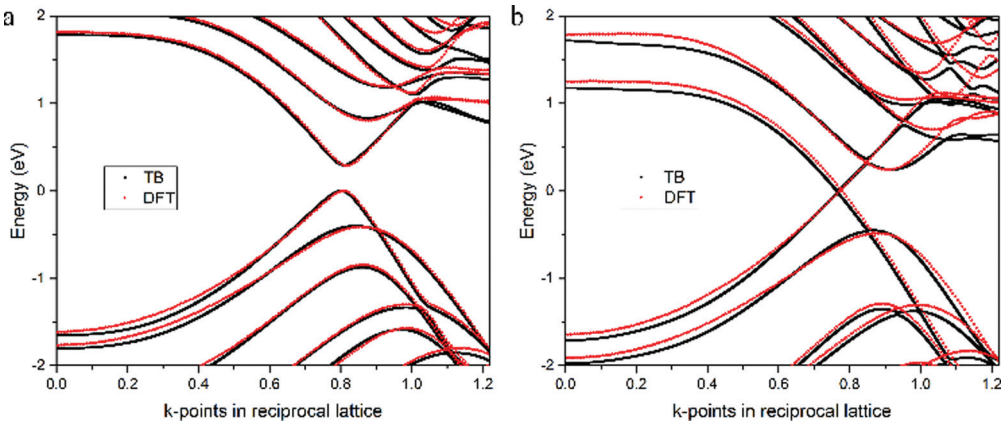

Fig. 3 (color online). Calculated band structures of (a) AB-stacked and (b) AA-stacked CEBG near the Fermi level using DFT data (red dotted lines) and TB models (black dotted lines).

phases of the pseudospins in different layers are not correlated and do not exhibit exclusive chirality. This point can be seen from the Berry phase, which is closely linked to the pseudospin. The Berry phase for a standing wave near a zig-zag is trivial, whether for single-layer or bilayer zig-zag ribbons.[26–29] After closing the edges, a non-trivial Berry phase of π appears for CEBG structures, which is different from the Berry phase of 2π of bilayer graphene.[30,31] This variation between bilayer graphene and CEBG will significantly influence the Hall conductance and provide direct evidence for quantum Hall effect experiments.

Our theory is valid for these three systems: bilayer graphene (with two open boundaries), folded graphene[32] (with one closed boundary), and CEBGs or collapsed nanotubes[33] (with no open boundaries). For bilayer graphene, the phases of the pseudospins in different layers are not correlated and do not exhibit exclusive chirality. After single-layer graphene is folded or its edges are closed, one can travel from the top layer to the bottom layer, which thus leads to interlayer interaction due to the opposite chirality of the pseudospin. The mechanism of the metal-to-semiconductor transition in collapsed armchair metallic tubes is the physical distinction between the two sublattices,[34,35] which is invalid for the other two systems.[36] Actually, this mechanism is just a special case of our theory. More generally, based on our theory, any bilayers with pseudospin of different chirality will exhibit a gap.[18] Indeed, gaps appear in bilayer graphene even in the absence of external magnetic and electric fields due to electron-electron interactions.[37–44] Compared with the gap caused by pseudospin interaction, this spontaneous gap, which is estimated to be of the order of 1 meV, is trivial. Therefore, the main features of our findings still remain the same.

We also plotted the density distribution of holes at the valence band maximum (VBM) and electrons at the conduction band minimum (CBM) of CEBGs in Fig. 4. The LE states of AA-stacked CEBG are distributed symmetrically, with higher densities around the center owing to interlayer coupling. However, for AB-stacked CEBG, the symmetrical distributions

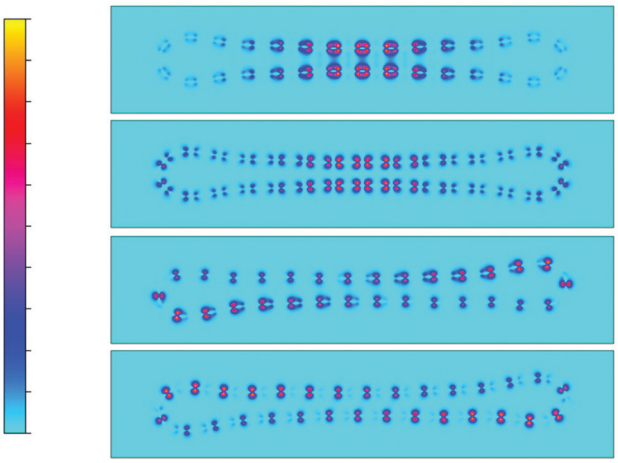

Fig. 4 (color online). Density of CBM electrons and VBM holes in AA-stacked CEBG and density of CBM electrons and VBM holes in AB-stacked CEBG (from top to bottom). The isosurface level is set to 0.0003. Red, yellow, purple, and blue colors indicate electron density from high to low.

of charge densities break down, giving VBM states on the top left wing and bottom right wing (\style) and CBM states on the top right wing and bottom left wing (/style). Obviously, such asymmetrical charge profiles are energetically favored over the symmetrical cases, which is due to the geometrical asymmetry in AB-stacked CEBG. This spatial separation of electrons and holes effectively forms a type II junction without impurity doping and provides the possibility of new charge separation mechanisms, as proposed by Wu *et al.* in tapered or strained silicon nanowires.[45,46]

Over many years of the development of semiconductor electronics, achieving charge separation has always been a critical requirement for the application in electronic or optoelectronic devices of p–n homojunctions or type II heterojunctions. Here, AB-stacked CEBG, which can also be referred to as a 'type-II homojunction', will avoid the technical hurdles of doping in

p–n homojunctions and also eliminate deficiencies caused by lattice mismatching at the interfaces in type II heterojunctions. In addition, compared with tapered or strained silicon nanowires, our CEBG models have more remarkable desirable properties owing to the high carrier mobility and high transparency of graphene. When it has geometrically separated charges and an opened band gap, AB-stacked CEBG can be used as a building block for developing future graphene-functionalized electronic devices, such as solar cells.

Here, as shown in Fig. 5a, we propose a multi-folded graphene model derived from AB-stacked CEBG. As expected, its energy spectrum has a finite band gap induced by pseudospin repulsion (see Fig. 5b). Moreover, the density distributions of VBM holes and CBM electrons in Fig. 5c and d show similar asymmetrical charge separation to that of AB-stacked CEBG, where the VBM holes are distributed in '\' style and the CBM electrons are distributed in '/' style. Fig. 5e illustrates an extremely simple way of harvesting solar energy with AB-stacked CEBG. In this graphene pseudospintronic model device, if illuminated by sunlight, electrons and holes will be activated separately to the folded edges and alternately layer by layer, owing to the chiral AB stacking. To facilitate the preparation of multi-layer folded graphene models, one can fold graphene flakes by introducing anisotropic surface curvature during the synthesis or transfer processes.[47] For example, graphene is first transferred onto a patterned metal substrate. Then, by etching the metal pattern, the graphene flakes collapse to form multi-folded features.

In summary, we have shown that AB-stacked CEBG exhibits appealing features such as band gap opening and spatial charge separation. The former originates from pseudospin interactions, whereas the latter arises from geometrical asymmetry. Concerning the daunting obstacles to opening the band gap in graphene, the present findings could boost the electronic properties of graphene-based devices and provide a novel way towards future pseudospin electronics for utilising the distinctive transport properties of graphene.

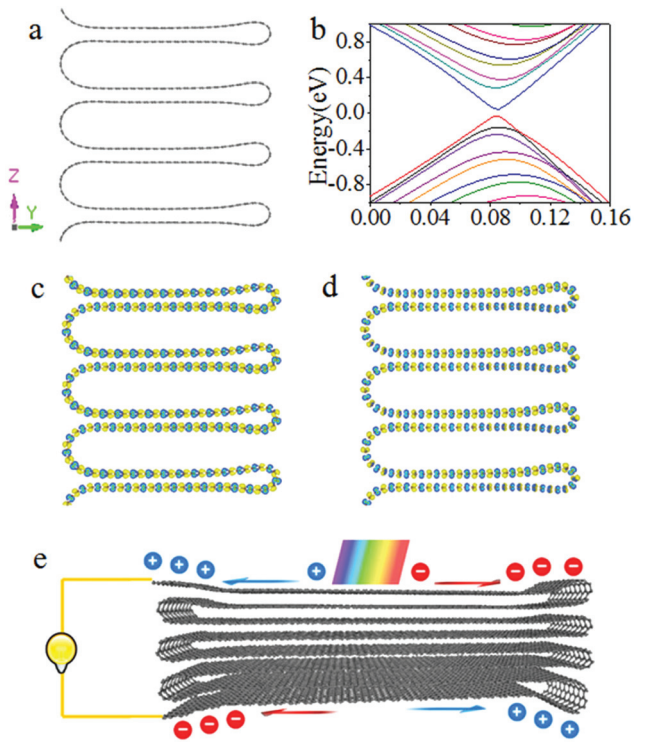

Fig. 5 (color online). (a) Model of multi-folded graphene, which is periodic along the *z*- and *x*-axes. (b) Calculated band structures of multi-folded graphene. Density of CBM electrons (c) and VBM holes (d) of multi-folded graphene. (e) Schematic of model device that harvests solar energy with multi-folded graphene. The isosurface level is set to 0.0003.

Acknowledgements

This research was supported by MOE under AcRF Tier 2 (MOE2012-T2-2-124) and AcRF Tier 3 (MOE2011-T3-1-005) in Singapore.

References

1 D. Elias, R. Nair, T. Mohiuddin, S. Morozov, P. Blake, M. Halsall, A. Ferrari, D. Boukhvalov, M. Katsnelson, A. Geim, *et al.*, *Science*, 2009, **323**, 610–613.
2 T. Ohta, A. Bostwick, T. Seyller, K. Horn and E. Rotenberg, *Science*, 2006, **313**, 951–954.
3 J. B. Oostinga, H. B. Heersche, X. Liu, A. F. Morpurgo and L. M. Vandersypen, *Nat. Mater.*, 2008, **7**, 151–157.
4 Y. Zhang, T.-T. Tang, C. Girit, Z. Hao, M. C. Martin, A. Zettl, M. F. Crommie, Y. R. Shen and F. Wang, *Nature*, 2009, **459**, 820–823.
5 Y.-W. Son, M. L. Cohen and S. G. Louie, *Phys. Rev. Lett.*, 2006, **97**, 216803.
6 L. Yang, C.-H. Park, Y.-W. Son, M. L. Cohen and S. G. Louie, *Phys. Rev. Lett.*, 2007, **99**, 186801.
7 X. Peng and R. Ahuja, *Nano Lett.*, 2008, **8**, 4464–4468.
8 S. Zhou, G.-H. Gweon, A. Fedorov, P. First, W. De Heer, D.-H. Lee, F. Guinea, A. C. Neto and A. Lanzara, *Nat. Mater.*, 2007, **6**, 770–775.
9 J. Berashevich and T. Chakraborty, *Phys. Rev. B: Condens. Matter*, 2009, **80**, 033404.
10 L. Liu and Z. Shen, *Appl. Phys. Lett.*, 2009, **95**, 252104.
11 X. Wang, X. Li, L. Zhang, Y. Yoon, P. K. Weber, H. Wang, J. Guo and H. Dai, *Science*, 2009, **324**, 768–771.
12 Z. Liu, K. Suenaga, P. J. Harris and S. Iijima, *Phys. Rev. Lett.*, 2009, **102**, 015501.
13 D. Zhan, L. Liu, Y. N. Xu, Z. H. Ni, J. X. Yan, C. Zhao and Z. X. Shen, *Sci. Rep.*, 2011, **1**, 12.
14 S. H. Abedinpour, M. Polini, A. MacDonald, B. Tanatar, M. Tosi and G. Vignale, *Phys. Rev. Lett.*, 2007, **99**, 206802.
15 H. Min, G. Borghi, M. Polini and A. H. MacDonald, *Phys. Rev. B: Condens. Matter*, 2008, **77**, 041407.

16 P. San-Jose, E. Prada, E. McCann and H. Schomerus, *Phys. Rev. Lett.*, 2009, **102**, 247204.
17 M. Trushin and J. Schliemann, *Phys. Rev. Lett.*, 2011, **107**, 156801.
18 G. Kresse and J. Hafner, *Phys. Rev. B: Condens. Matter*, 1993, **47**, 558.
19 G. Kresse and J. Hafner, *Phys. Rev. B: Condens. Matter*, 1993, **48**, 13115.
20 G. Kresse and J. Furthmuller, *Comput. Mater. Sci.*, 1996, **6**, 15.
21 J. P. Perdew, K. Burke and M. Ernzerhof, *Phys. Rev. Lett.*, 1996, **77**, 3865.
22 M. Ouyang, J.-L. Huang, C. L. Cheung and C. M. Lieber, *Science*, 2001, **292**, 702–705.
23 J. Klimeš, D. R. Bowler and A. Michaelides, *Phys. Rev. B: Condens. Matter*, 2011, **83**, 195131.
24 M. S. Hybertsen and S. G. Louie, *Phys. Rev. B: Condens. Matter*, 1986, **34**, 5390.
25 A. Marini, C. Hogan, M. Grüning and D. Varsano, *Comput. Phys. Commun.*, 2009, **180**(8), 1392–1403.
26 J. Feng, L. Qi, J. Y. Huang and J. Li, *Phys. Rev. B: Condens. Matter*, 2009, **80**, 165407.
27 C.-H. Park and N. Marzari, *Phys. Rev. B: Condens. Matter*, 2011, **84**, 205440.
28 K.-I. Sasaki, M. Yamamoto, S. Murakami, R. Saito, M. S. Dresselhaus, K. Takai, T. Mori, T. Enoki and K. Wakabayashi, *Phys. Rev. B: Condens. Matter*, 2009, **80**, 155450.
29 K.-I. Sasaki, K. Wakabayashi and T. Enoki, *New J. Phys.*, 2010, **12**, 083023.
30 E. McCann and V. I. Falárko, *Phys. Rev. Lett.*, 2006, **96**, 086805.
31 K. Novoselov, E. McCann, S. Morozov, V. I. Falárko, M. Katsnelson, U. Zeitler, D. Jiang, F. Schedin and A. Geim, *Nat. Phys.*, 2006, **2**, 177–180.
32 D. Rainis, F. Taddei, M. Polini, G. León, F. Guinea and V. I. Falárko, *Phys. Rev. B: Condens. Matter*, 2011, **83**, 165403.
33 N. Chopra, L. Benedict, V. Crespi, M. Cohen, S. Louie and A. Zetti, *Nature*, 1995, **377**, 135–138.
34 P. E. Lammert, P. Zhang and V. H. Crespi, *Phys. Rev. Lett.*, 2000, **84**, 2453–2456.
35 J.-Q. Lu, J. Wu, W. Duan, F. Liu, B.-F. Zhu and B.-L. Gu, *Phys. Rev. Lett.*, 2003, **90**, 156601.
36 J.-Q. Lu, J. Wu, W. Duan, B.-L. Gu and H. Johnson, *J. Appl. Phys.*, 2005, **97**, 114314.
37 H. Min, G. Borghi, M. Polini and A. H. MacDonald, *Phys. Rev. B: Condens. Matter*, 2008, **77**, 041407.
38 R. Nandkishore and L. Levitov, *Phys. Rev. Lett.*, 2010, **104**, 156803.
39 F. Zhang, J. Jung, G. A. Fiete, Q. Niu and A. H. MacDonald, *Phys. Rev. Lett.*, 2011, **106**, 156801.
40 Y. Lemonik, I. Aleiner, C. Toke and V. Falárko, *Phys. Rev. B: Condens. Matter*, 2010, **82**, 201408.
41 J. Martin, B. E. Feldman, R. T. Weitz, M. T. Allen and A. Yacoby, *Phys. Rev. Lett.*, 2010, **105**, 256806.
42 W. Bao, Z. Zhao, H. Zhang, G. Liu, P. Kratz, L. Jing, J. Velasco Jr., D. Smirnov and C. N. Lau, *Phys. Rev. Lett.*, 2010, **105**, 246601.
43 R. T. Weitz, M. Allen, B. Feldman, J. Martin and A. Yacoby, *Science*, 2010, **330**, 812–816.
44 A. Mayorov, D. Elias, M. Mucha-Kruczynski, R. Gorbachev, T. Tudorovskiy, A. Zhukov, S. Morozov, M. Katsnelson, A. Geim and K. Novoselov, *Science*, 2011, **333**, 860–863.
45 Z. Wu, J. Neaton and J. C. Grossman, *Phys. Rev. Lett.*, 2008, **100**, 246804.
46 Z. Wu, J. Neaton and J. C. Grossman, *Nano Lett.*, 2009, **9**, 2418–2422.
47 K. Kim, Z. Lee, B. D. Malone, K. T. Chan, B. Alemán, W. Regan, W. Gannett, M. F. Crommie, M. L. Cohen and A. Zettl, *Phys. Rev. B: Condens. Matter*, 2011, **83**, 245433.

